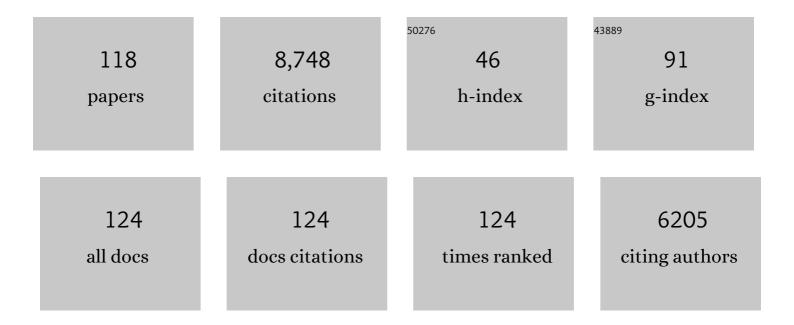
Dmitriy A Yablonskiy

List of Publications by Year in descending order

Source: https://exaly.com/author-pdf/8569185/publications.pdf Version: 2024-02-01



#	Article	IF	CITATIONS
1	Theory of NMR signal behavior in magnetically inhomogeneous tissues: The static dephasing regime. Magnetic Resonance in Medicine, 1994, 32, 749-763.	3.0	1,086
2	Water proton MR properties of human blood at 1.5 Tesla: Magnetic susceptibility,T1,T2,T*2, and non-Lorentzian signal behavior. Magnetic Resonance in Medicine, 2001, 45, 533-542.	3.0	421
3	Quantitative BOLD: Mapping of human cerebral deoxygenated blood volume and oxygen extraction fraction: Default state. Magnetic Resonance in Medicine, 2007, 57, 115-126.	3.0	335
4	Quantitative in vivo assessment of lung microstructure at the alveolar level with hyperpolarized 3He diffusion MRI. Proceedings of the National Academy of Sciences of the United States of America, 2002, 99, 3111-3116.	7.1	325
5	Modeling dendrite density from magnetic resonance diffusion measurements. NeuroImage, 2007, 34, 1473-1486.	4.2	296
6	MR imaging of diffusion of3He gas in healthy and diseased lungs. Magnetic Resonance in Medicine, 2000, 44, 174-179.	3.0	292
7	Biophysical mechanisms of phase contrast in gradient echo MRI. Proceedings of the National Academy of Sciences of the United States of America, 2009, 106, 13558-13563.	7.1	255
8	Theory and application of static field inhomogeneity effects in gradient-echo imaging. Journal of Magnetic Resonance Imaging, 1997, 7, 266-279.	3.4	254
9	Neurite density from magnetic resonance diffusion measurements at ultrahigh field: Comparison with light microscopy and electron microscopy. NeuroImage, 2010, 49, 205-216.	4.2	245
10	Evidence for Adult Lung Growth in Humans. New England Journal of Medicine, 2012, 367, 244-247.	27.0	237
11	Quantitation of intrinsic magnetic susceptibility-related effects in a tissue matrix. Phantom study. Magnetic Resonance in Medicine, 1998, 39, 417-428.	3.0	224
12	Statistical model for diffusion attenuated MR signal. Magnetic Resonance in Medicine, 2003, 50, 664-669.	3.0	220
13	Hyperpolarized ³ He diffusion MRI and histology in pulmonary emphysema. Magnetic Resonance in Medicine, 2006, 56, 1293-1300.	3.0	191
14	On the nature of the NAA diffusion attenuated MR signal in the central nervous system. Magnetic Resonance in Medicine, 2004, 52, 1052-1059.	3.0	149
15	Quantification of lung microstructure with hyperpolarized 3He diffusion MRI. Journal of Applied Physiology, 2009, 107, 1258-1265.	2.5	139
16	Theoretical models of the diffusion weighted MR signal. NMR in Biomedicine, 2010, 23, 661-681.	2.8	133
17	Fatty liver in familial hypobetalipoproteinemia: triglyceride assembly into VLDL particles is affected by the extent of hepatic steatosis. Journal of Lipid Research, 2003, 44, 470-478.	4.2	127
18	Validation of oxygen extraction fraction measurement by qBOLD technique. Magnetic Resonance in Medicine, 2008, 60, 882-888.	3.0	124

#	Article	IF	CITATIONS
19	Fatty liver in familial hypobetalipoproteinemia. Journal of Lipid Research, 2004, 45, 941-947.	4.2	121
20	Blood oxygenation levelâ€dependent (BOLD)â€based techniques for the quantification of brain hemodynamic and metabolic properties – theoretical models and experimental approaches. NMR in Biomedicine, 2013, 26, 963-986.	2.8	116
21	Rapid imaging of hyperpolarized gas using EPI. Magnetic Resonance in Medicine, 1999, 42, 507-514.	3.0	104
22	In vivo validation of the bold mechanism: A review of signal changes in gradient echo functional MRI in the presence of flow. International Journal of Imaging Systems and Technology, 1995, 6, 153-163.	4.1	99
23	Hyperpolarized3He gas production and MR imaging of the lung. Concepts in Magnetic Resonance, 2001, 13, 277-293.	1.3	98
24	Voxel spread function method for correction of magnetic field inhomogeneity effects in quantitative gradientâ€echoâ€based MRI. Magnetic Resonance in Medicine, 2013, 70, 1283-1292.	3.0	98
25	Theoretical model of temperature regulation in the brain during changes in functional activity. Proceedings of the National Academy of Sciences of the United States of America, 2006, 103, 12144-12149.	7.1	93
26	Homonuclear J coupling effects in volume localized NMR spectroscopy: Pitfalls and solutions. Magnetic Resonance in Medicine, 1998, 39, 169-178.	3.0	92
27	Protein-induced water 1H MR frequency shifts: Contributions from magnetic susceptibility and exchange effects. Journal of Magnetic Resonance, 2010, 202, 102-108.	2.1	83
28	An MRI method for measuringT2 in the presence of static and RF magnetic field Inhomogeneities. Magnetic Resonance in Medicine, 1997, 37, 872-876.	3.0	82
29	Biophysical mechanisms of MRI signal frequency contrast in multiple sclerosis. Proceedings of the National Academy of Sciences of the United States of America, 2012, 109, 14212-14217.	7.1	81
30	How the body controls brain temperature: the temperature shielding effect of cerebral blood flow. Journal of Applied Physiology, 2006, 101, 1481-1488.	2.5	80
31	Effects of Restricted Diffusion on MR Signal Formation. Journal of Magnetic Resonance, 2002, 157, 92-105.	2.1	77
32	On the role of neuronal magnetic susceptibility and structure symmetry on gradient echo MR signal formation. Magnetic Resonance in Medicine, 2014, 71, 345-353.	3.0	75
33	Hyperpolarized ³ He MR Imaging: Physiologic Monitoring Observations and Safety Considerations in 100 Consecutive Subjects. Radiology, 2008, 248, 655-661.	7.3	74
34	Extracellular apparent diffusion in rat brain. Magnetic Resonance in Medicine, 2001, 45, 801-810.	3.0	70
35	Long-range diffusion of hyperpolarized 3He in explanted normal and emphysematous human lungs via magnetization tagging. Journal of Applied Physiology, 2005, 99, 1992-1997.	2.5	67
36	Gaussian approximation in the theory of MR signal formation in the presence of structure-specific magnetic field inhomogeneities. Journal of Magnetic Resonance, 2003, 163, 236-247.	2.1	66

#	Article	IF	CITATIONS
37	In Vivo Detection of Acinar Microstructural Changes in Early Emphysema with3He Lung Morphometry. Radiology, 2011, 260, 866-874.	7.3	66
38	Magnetization tagging decay to measure long-range3He diffusion in healthy and emphysematous canine lungs. Magnetic Resonance in Medicine, 2004, 51, 1002-1008.	3.0	61
39	Dynamic echo planar MR imaging of lung ventilation with hyperpolarized3He in normal subjects and patients with severe emphysema. NMR in Biomedicine, 2000, 13, 176-181.	2.8	58
40	Lung morphometry with hyperpolarized ¹²⁹ Xe: Theoretical background. Magnetic Resonance in Medicine, 2012, 67, 856-866.	3.0	57
41	Separation of cellular and BOLD contributions to T2* signal relaxation. Magnetic Resonance in Medicine, 2016, 75, 606-615.	3.0	57
42	Gaussian approximation in the theory of MR signal formation in the presence of structure-specific magnetic field inhomogeneities. Effects of impermeable susceptibility inclusions. Journal of Magnetic Resonance, 2004, 167, 56-67.	2.1	55
43	Quantitation ofT2′ anisotropic effects on magnetic resonance bone mineral density measurement. Magnetic Resonance in Medicine, 1997, 37, 214-221.	3.0	54
44	On the role of physiological fluctuations in quantitative gradient echo MRI: implications for GEPCI, QSM, and SWI. Magnetic Resonance in Medicine, 2015, 73, 195-203.	3.0	53
45	In vivo detection of microstructural correlates of brain pathology in preclinical and early Alzheimer Disease with magnetic resonance imaging. NeuroImage, 2017, 148, 296-304.	4.2	52
46	Gradient Echo Plural Contrast Imaging — Signal model and derived contrasts: T2*, T1, Phase, SWI, T1f, FST2*and T2*-SWI. NeuroImage, 2012, 60, 1073-1082.	4.2	50
47	Theory of FID NMR Signal Dephasing Induced by Mesoscopic Magnetic Field Inhomogeneities in Biological Systems. Journal of Magnetic Resonance, 2001, 151, 107-117.	2.1	49
48	In vivo lung morphometry with hyperpolarized 3He diffusion MRI in canines with induced emphysema: disease progression and comparison with computed tomography. Journal of Applied Physiology, 2007, 102, 477-484.	2.5	49
49	Body and brain temperature coupling: the critical role of cerebral blood flow. Journal of Comparative Physiology B: Biochemical, Systemic, and Environmental Physiology, 2009, 179, 701-710.	1.5	48
50	Quantitative phenomenological model of the BOLD contrast mechanism. Journal of Magnetic Resonance, 2011, 212, 17-25.	2.1	48
51	19F MR imaging of ventilation and diffusion in excised lungs. Magnetic Resonance in Medicine, 2005, 54, 577-585.	3.0	45
52	Hyperpolarized 3He and perfluorocarbon gas diffusion MRI of lungs. Progress in Nuclear Magnetic Resonance Spectroscopy, 2006, 48, 63-83.	7.5	45
53	Improved calibration technique for in vivo proton MRS thermometry for brain temperature measurement. Magnetic Resonance in Medicine, 2008, 60, 536-541.	3.0	44
54	Genetically defined cellular correlates of the baseline brain MRI signal. Proceedings of the National Academy of Sciences of the United States of America, 2018, 115, E9727-E9736.	7.1	43

#	Article	IF	CITATIONS
55	Magnetic susceptibility induced white matter MR signal frequency shifts—experimental comparison between Lorentzian sphere and generalized Lorentzian approaches. Magnetic Resonance in Medicine, 2014, 71, 1251-1263.	3.0	42
56	Generalized Lorentzian Tensor Approach (GLTA) as a biophysical background for quantitative susceptibility mapping. Magnetic Resonance in Medicine, 2015, 73, 757-764.	3.0	41
57	Direct comparison of ¹²⁹ <scp>X</scp> e diffusion measurements with quantitative histology in human lungs. Magnetic Resonance in Medicine, 2017, 77, 265-272.	3.0	39
58	On the role of anesthesia on the body/brain temperature differential in rats. Journal of Thermal Biology, 2004, 29, 599-603.	2.5	38
59	Assessment of Regional Lung Function with Multivolume ¹ H MR Imaging in Health and Obstructive Lung Disease: Comparison with ³ He MR Imaging. Radiology, 2014, 273, 580-590.	7.3	38
60	Combined MR proton lung perfusion/angiography and helium ventilation: Potential for detecting pulmonary emboli and ventilation defects. Magnetic Resonance in Medicine, 2002, 47, 433-438.	3.0	36
61	Image artifacts in very low magnetic field MRI: The role of concomitant gradients. Journal of Magnetic Resonance, 2005, 174, 279-286.	2.1	35
62	3He Diffusion MRI of the Lung1. Academic Radiology, 2005, 12, 1406-1413.	2.5	35
63	Effects of diffusion time on shortâ€range hyperpolarized ³ He diffusivity measurements in emphysema. Journal of Magnetic Resonance Imaging, 2009, 30, 801-808.	3.4	34
64	Imaging lung microstructure in mice with hyperpolarized ³ He diffusion MRI. Magnetic Resonance in Medicine, 2011, 65, 620-626.	3.0	34
65	Experimental evidence of age-related adaptive changes in human acinar airways. Journal of Applied Physiology, 2016, 120, 159-165.	2.5	34
66	Theoretical limits on brain cooling by external head cooling devices. European Journal of Applied Physiology, 2007, 101, 41-49.	2.5	33
67	Probing lung microstructure with hyperpolarized noble gas diffusion MRI: theoretical models and experimental results. Magnetic Resonance in Medicine, 2014, 71, 486-505.	3.0	33
68	Albumin-binding MR blood pool agents as MRI contrast agents in an intracranial mouse glioma model. Magnetic Resonance in Medicine, 2003, 49, 586-590.	3.0	32
69	Natural linewidth chemical shift imaging (NL-CSI). Magnetic Resonance in Medicine, 2006, 56, 7-18.	3.0	32
70	In vivo quantitative evaluation of brain tissue damage in multiple sclerosis using gradient echo plural contrast imaging technique. Neurolmage, 2010, 51, 1089-1097.	4.2	32
71	Cerebral metabolic rate in hypercapnia: Controversy continues. Journal of Cerebral Blood Flow and Metabolism, 2011, 31, 1502-1503.	4.3	32
72	Gradient echo magnetic resonance imaging correlates with clinical measures and allows visualization of veins within multiple sclerosis lesions. Multiple Sclerosis Journal, 2014, 20, 349-355.	3.0	30

#	Article	IF	CITATIONS
73	Effects of biological tissue structural anisotropy and anisotropy of magnetic susceptibility on the gradient echo MRI signal phase: theoretical background. NMR in Biomedicine, 2017, 30, e3655.	2.8	30
74	Role of collateral paths in long-range diffusion in lungs. Journal of Applied Physiology, 2008, 104, 1495-1503.	2.5	28
75	Biophysical mechanisms of myelinâ€induced water frequency shifts. Magnetic Resonance in Medicine, 2014, 71, 1956-1958.	3.0	28
76	Optimal decay rate constant estimates from phased array data utilizing joint Bayesian analysis. Journal of Magnetic Resonance, 2009, 198, 49-56.	2.1	27
77	On the relationship between cellular and hemodynamic properties of the human brain cortex throughout adult lifespan. NeuroImage, 2016, 133, 417-429.	4.2	27
78	Absence of fatty liver in familial hypobetalipoproteinemia linked to chromosome 3p21. Metabolism: Clinical and Experimental, 2005, 54, 682-688.	3.4	26
79	The Role of Collateral Paths in Long-range Diffusion of 3He in Lungs. Academic Radiology, 2008, 15, 675-682.	2.5	24
80	Transmembrane dynamics of water exchange in human brain. Magnetic Resonance in Medicine, 2012, 67, 562-571.	3.0	24
81	Detection and quantification of regional cortical gray matter damage in multiple sclerosis utilizing gradient echo MRI. Neurolmage: Clinical, 2015, 9, 164-175.	2.7	22
82	In vivo lung morphometry with hyperpolarized ³ He diffusion MRI: Reproducibility and the role of diffusion-sensitizing gradient direction. Magnetic Resonance in Medicine, 2015, 73, 1252-1257.	3.0	22
83	In vivo lung morphometry with accelerated hyperpolarized ³ He diffusion MRI: A preliminary study. Magnetic Resonance in Medicine, 2015, 73, 1609-1614.	3.0	21
84	Optimization strategies for evaluation of brain hemodynamic parameters with qBOLD technique. Magnetic Resonance in Medicine, 2013, 69, 1034-1043.	3.0	20
85	Lorentz sphere versus generalized Lorentzian approach: What would lorentz say about it?. Magnetic Resonance in Medicine, 2014, 72, 4-7.	3.0	20
86	Diffusion lung imaging with hyperpolarized gas MRI. NMR in Biomedicine, 2017, 30, e3448.	2.8	20
87	In vivo evaluation of heme and non-heme iron content and neuronal density in human basal ganglia. NeuroImage, 2021, 235, 118012.	4.2	19
88	How accurately can the parameters from a model of anisotropic 3He gas diffusion in lung acinar airways be estimated? Bayesian view. Journal of Magnetic Resonance, 2007, 184, 62-71.	2.1	16
89	Deep learning using a biophysical model for robust and accelerated reconstruction of quantitative, artifactâ€free and denoised images. Magnetic Resonance in Medicine, 2020, 84, 2932-2942.	3.0	15
90	Limbic system damage in MS: MRI assessment and correlations with clinical testing. PLoS ONE, 2017, 12, e0187915.	2.5	14

#	Article	IF	CITATIONS
91	Single scan quantitative gradient recalled echo MRI for evaluation of tissue damage in lesions and normal appearing gray and white matter in multiple sclerosis. Journal of Magnetic Resonance Imaging, 2019, 49, 487-498.	3.4	14
92	Feasibility of combining MR perfusion, angiography, and 3He ventilation imaging for evaluation of lung function in a porcine model1. Academic Radiology, 2005, 12, 202-209.	2.5	13
93	Emphysema Quantification in Inflation-Fixed Lungs Using Low-Dose Computed Tomography and 3He Magnetic Resonance Imaging. Journal of Computer Assisted Tomography, 2010, 34, 773-779.	0.9	11
94	Lorentzian effects in magnetic susceptibility mapping of anisotropic biological tissues. Journal of Magnetic Resonance, 2018, 292, 129-136.	2.1	11
95	Commentary on "The influence of lung airways branching structure and diffusion time on measurements and models of short-range 3He gas MR diffusion― Journal of Magnetic Resonance, 2014, 239, 139-142.	2.1	10
96	Subcomponents of brain T2* relaxation in schizophrenia, bipolar disorder and siblings: A Gradient Echo Plural Contrast Imaging (GEPCI) study. Schizophrenia Research, 2015, 169, 36-45.	2.0	10
97	Probing lung microstructure with hyperpolarized ³ He gradient echo MRI. NMR in Biomedicine, 2014, 27, 1451-1460.	2.8	9
98	What makes a good pediatric transplant lung: Insights from in vivo lung morphometry with hyperpolarized ³ He magnetic resonance imaging. Pediatric Transplantation, 2017, 21, e12886.	1.0	9
99	Learningâ€based motion artifact removal networks for quantitative R2â^— mapping. Magnetic Resonance in Medicine, 2022, 88, 106-119.	3.0	9
100	Commentaries on Viewpoint: Unresolved mysteries. Journal of Applied Physiology, 2012, 113, 1948-1949.	2.5	7
101	A Novel Gradient Echo Plural Contrast Imaging Method Detects Brain Tissue Abnormalities in Patients With TBI Without Evident Anatomical Changes on Clinical MRI: A Pilot Study. Military Medicine, 2019, 184, 218-227.	0.8	7
102	Detection of cortical lesions in multiple sclerosis: A new imaging approach. Multiple Sclerosis Journal - Experimental, Translational and Clinical, 2015, 1, 205521731560646.	1.0	6
103	Simultaneous multiâ€angular relaxometry of tissue with MRI (SMART MRI): Theoretical background and proof of concept. Magnetic Resonance in Medicine, 2017, 77, 1296-1306.	3.0	6
104	In vivo evolution of biopsyâ€proven inflammatory demyelination quantified by R2t* mapping. Annals of Clinical and Translational Neurology, 2020, 7, 1055-1060.	3.7	6
105	The Role of the Human Brain Neuron–Glia–Synapse Composition in Forming Resting-State Functional Connectivity Networks. Brain Sciences, 2021, 11, 1565.	2.3	6
106	Phaseâ€sensitive B ₁ mapping: Effects of relaxation and RF spoiling. Magnetic Resonance in Medicine, 2018, 80, 101-111.	3.0	4
107	Quantitative Gradient Echo MRI Identifies Dark Matter as a New Imaging Biomarker of Neurodegeneration that Precedes Tissue Atrophy in Early Alzheimer's Disease. Journal of Alzheimer's Disease, 2022, 85, 905-924.	2.6	3

MR imaging of diffusion of 3He gas in healthy and diseased lungs. , 2000, 44, 174.

2

#	Article	IF	CITATIONS
109	Stronger Microstructural Damage Revealed in Multiple Sclerosis Lesions With Central Vein Sign by Quantitative Gradient Echo MRI. Journal of Central Nervous System Disease, 2022, 14, 117957352210848.	1.9	2
110	Tissue damage detected by quantitative gradient echo MRI correlates with clinical progression in non-relapsing progressive MS. Multiple Sclerosis Journal, 2022, 28, 1515-1525.	3.0	2
111	HYPERPOLARIZED 3HELIUM MAGNETIC RESONANCE IMAGING: SAFETY CONSIDERATIONS AND PHYSIOLOGIC MONITORING. Chest, 2007, 132, 525B.	0.8	1
112	Reply to Verbanck and Paiva. Journal of Applied Physiology, 2009, 106, 1024-1024.	2.5	0
113	[P2–393]: GRADIENT ECHO PLURAL CONTRAST MRI PROVIDES NEW SURROGATE MARKERS OF BRAIN PATHOLOGY IN ALZHEIMER's DISEASE. Alzheimer's and Dementia, 2017, 13, P780.	0.8	0
114	[ICâ€Pâ€169]: GRADIENT ECHO PLURAL CONTRAST MRI PROVIDES NEW SURROGATE MARKERS OF BRAIN PATHOLOGY IN ALZHEIMER's DISEASE. Alzheimer's and Dementia, 2017, 13, P127.	0.8	0
115	Theoretical models of diffusion-attenuated magnetic resonance signal in biological tissues. Low Temperature Physics, 2020, 46, 768-772.	0.6	0
116	Measuring Collateral Pathways in Health via 3 He MRI. FASEB Journal, 2008, 22, 763.9.	0.5	0
117	Function and Microstructure by Hyperpolarized Gas MRI. , 2014, , 247-267.		0
118	Linking gradient echo plural contrast imaging metrics of tissue microstructure with Alzheimer disease. , 2020, , 507-519.		0